Mass Transfer Effects in CO_2 Reduction on Cu Nanowire Electrocatalysts

Journal:	*Catalysis Science & Technology*
Manuscript ID	CY-ART-02-2018-000372.R2
Article Type:	Paper
Date Submitted by the Author:	03-Apr-2018
Complete List of Authors:	Raciti, David; Johns Hopkins University, Chemical and Biomolecular Engineering Mao, Mark; Johns Hopkins University, Chemical and Biomolecular Engineering Park, Jun Ha; Johns Hopkins University, Chemical and Biomolecular Engineering Wang, Chao; Johns Hopkins University, Chemical and Biomolecular Engineering

SCHOLARONE™
Manuscripts

Catalysis Science & Technology

ARTICLE

Mass Transfer Effects in CO_2 Reduction on Cu Nanowire Electrocatalysts

Received 00th January 20xx,
Accepted 00th January 20xx

DOI: 10.1039/x0xx00000x

www.rsc.org/

David Raciti,[a] Mark Mao,[a] Jun Ha Park,[a] Chao Wang[a,] *

Significant interests have risen in the development of catalytic nanomaterials for the electroreduction of CO_2. While extensive studies have been reported on tuning of surface structures to improve the chemical kinetics, less attention has been paid to the mass transfer effects in the CO_2 reduction reaction on nanoscale electrocatalysts. We report here an systematic investigation of CO_2 electroreduction on highly dense Cu nanowires, with the focus placed on practical high-flux conditions. Mass transfer effects are found to play an important role in this case, giving rise to diffusion-limited CO_2 reduction activity and selectivity. By correlating the observed transport phenomena to the CO_2 conversion rate calculated from the experimental data and the surface concentration of CO_2 on the nanowires derived from modeling, an upper limit is revealed for the CO_2 conversion rate on the nanostructured electrodes, which also causes the drop in Faradaic efficiency of CO_2 reduction at large current densities. Our work emphasizes the necessity of considering mass transfer effects in the design of advanced electrocatalysts for CO_2 reduction as well as for understanding their structure-performance relationships.

Introduction

Electrochemical reduction of carbon dioxide (CO_2) has garnered increasing interest as a promising solution for artificial carbon recycling and solar-fuel conversion.[1–3] With water as the proton source, this process can convert the greenhouse gas, CO_2, into carbon monoxide, methane, ethanol, ethylene or other (oxygenated) hydrocarbons; e.g., $CO_2 + H_2O + 2e^- \rightarrow CO + 2OH^-$ and $2CO_2 + 8H_2O + 12e^- \rightarrow C_2H_4 + 12OH^-$. These species can either be directly used as fuels, such as ethanol for substitution of gasoline, or fed into chemical plants to make more valuable products (e.g., various polymers from ethylene). Despite the great potential, electrochemical reduction of CO_2 has been challenged by the lack of efficient electrocatalysts. Even copper (Cu), the most active metal for reducing CO_2 to hydrocarbons known to date, still requires highly negative potentials of about -1.0 V versus reversible hydrogen electrode (RHE; the same in the following discussion unless otherwise specified) to produce valuable products such as ethylene and ethanol.[4–6] Additionally, the undesired byproduct, hydrogen, is still produced at significant amounts.[6,7]

Extensive studies on Cu-based electrocatalysts have shown that the catalytic activity and product distribution are dependent on the electrode morphologies,[8–12] compositions [13,14] and surface structures.[15–21] Besides the catalyst structure, electrocatalysis of CO_2 is also dependent on the electrolyte and CO_2 partial pressure.[5,22–26] While protons are readily available in aqueous solutions via water reduction, the supply of reactant to the electrode surface is limited by the concentration and diffusivity of dissolved CO_2 molecules, which places a hurdle on the current density and efficiency of CO_2 reduction.[22,24] Moreover, the reduction of CO_2 and evolution of H_2, produces hydroxide anions (OH^-) and raises the local pH on the electrode surface. The high local pH near the electrode surface could be detrimental to electrolysis of CO_2, as it shifts the equilibrium of CO_2 hydrolysis toward (bi)carbonates and further reduces the flux of CO_2 molecules attainable by the catalyst surface.[22,26] The early work on polycrystalline Cu electrodes (Cu-poly, in 0.1 M $KHCO_3$) by Hori *et al.* shows monotonic increase of Faradaic efficiency (FE) for CO_2 reduction, namely decrease of FE_{H2}, in the potential region from −0.4 to −1.1 V,[5] but a more recent study on Cu-poly (also in in 0.1 M $KHCO_3$) by Jaramillo *et al.* reveals that the FE of hydrogen evolution (FE_{H2}) reaches a minimum at ca. −1.1 V and then increase at more negative potentials.[27] The minimum in FE_{H2}, or maximal FE_{CO2}, is likely a result of the interplay between chemical kinetics on the surface and transport of CO_2 toward the catalyst surface: in the low-overpotential region, the electrocatalytic performance is more determined by the kinetic competition of the CO_2 reduction and hydrogen evolution reaction pathways, with the former becoming more favorable at more negative potentials;[21,28,29] on the other side, mass transfer plays a more important role at more elevated overpotentials and places a limit on the efficiency of CO_2

[a] Department of Chemical and Biomolecular Engineering, Johns Hopkins University, Baltimore, Maryland 21218
* Email: chaowang@jhu.edu
Electronic Supplementary Information (ESI) available: [details of any supplementary information available should be included here]. See DOI: 10.1039/x0xx00000x

This journal is © The Royal Society of Chemistry 20xx

Please do not adjust margins

reduction.[22,24,30] However, it is noticed that most of the previous discussions on mass transfer and local pH effects are based on electrocatalytic studies at fixed potentials [5,23,24,26] and/or with low-surface-area (e.g., extended-surface) electrodes.[5,22,24–26]. It largely remains elusive how the mass transfer effects correlate to the nanostructures of high-surface-area electrocatalysts, where the supply of CO_2 could play a more vital role in determining the catalytic performance owing to the large current densities.[8,10,12,31]

Here we report on the investigation of mass transfer effects in CO_2 reduction by using highly dense Cu nanowires as the electrocatalysts. The Cu nanowires were synthesized by reducing CuO nanowires grown on Cu mesh, either by applying a cathodic electrochemical potential or by thermal annealing in the presence of hydrogen. Our previous reports have shown that the electrochemically reduced Cu nanowires are highly active for CO_2 reduction, favoring the production of CO and formate at potentials more positive than -0.5 V.[10,32] In this work, we aim to systematically study the reduction of CO_2 in the high-overpotential region, i.e., potentials more negative than -0.5 V, where the transport phenomena become more pronounced compared to lower overpotentials. The dependence of catalytic activity and selectivity on the electrode potential are systematically evaluated on three types of Cu nanowires with different dimensions and surface roughness factors. The catalytic performance of each catalyst is correlated to the CO_2 conversion rate calculated from the experimental data and the surface concentration of CO_2 on the nanowires derived from transport modeling, where the effects of mass transfer on CO_2 reduction electrocatalysis are discussed.

Experimental

Synthesis of Cu Nanowires. Cu grid (100 mesh) was washed in 0.1 M HCl and then several times in DI H_2O. After drying in vacuum, the mesh was treated at 585-600 °C in air for 8 hours. Electrochemical reduction at –0.4 V was used to convert CuO nanowires to Cu nanowires. Reduction of CuO was monitored by recording the cathodic current and was deemed complete when a steady state current had been achieved.[10] Forming gas reduced nanowires (FGR) were synthesized by annealing CuO nanowires at 150 °C for 15h (HR-150) and 300 °C for 15h (HR-300 (15h)) while passing 10 sccm 5% H_2/Ar through a gas tube. The complete reduction of each sample was verified by X-Ray diffraction (XRD) post reduction treatment (Figure S1).

Material Characterization. SEM images were collected on a JEOL JSM-6700F field-emission scanning electron microscope. A field-emission Phillips CM300-FEG (300 kV) was used for TEM imaging. XRD patterns were collected on a PANalytical X'pert^3 Powder X-Ray Diffractometer equipped with a Cu K_α source (λ=0.15406).

Electrochemical Studies. The electroreduction of CO_2 was studied in 0.1 M $KHCO_3$ using a liquid and gas-tight custom-made electrolysis cell equipped with an Autolab 302 potentiostat (Metrohm). The electrolyte was purged with CO_2 at a rate of 20 sccm for 10 minutes prior and throughout the 1-hour duration of the measurement. To prevent oxidation of products at the anode, an anion exchange membrane from Selemion was used to separate the two compartments. The reference electrode (Ag/AgCl from BASi) was located in the cathode compartment. A piece of Pt mesh was used as the counter electrode in the anode compartment. Gas products were sampled periodically via a gas chromatography coupled to a mass spectrometer (Shimadzu GCMS-QP2010 SE). This method has relatively large uncertainty for measuring the concentration of H_2. The previous study has shown that the uncertainty in FE_{H2} can be up to ~10%.[10] Liquid products were analyzed at the end of each potential by collecting an aliquot of the electrolyte and using nuclear magnetic resonance (NMR, Bruker Advance 300 MHz) spectroscopy. An 85% iR drop correction was implemented via Autolab software.

Double-layer capacitance was measured to estimate the surface roughness and electrochemically active surface area (ECSA) of the Cu nanowires by recording cyclic voltammograms (CVs) in a non-Faradaic potential region (Figure S2).[10] The capacitances were compared and standardized versus a polycrystalline Cu disk to derive the surface roughness factors (Table S1).[8] The current densities per geometric area of the electrode (J_{tot} and J_{CO2}) were divided by the surface roughness factor to find out the specific activities (e.g., j_{tot} and j_{CO2}) as discussed in the text.

Results and Discussion

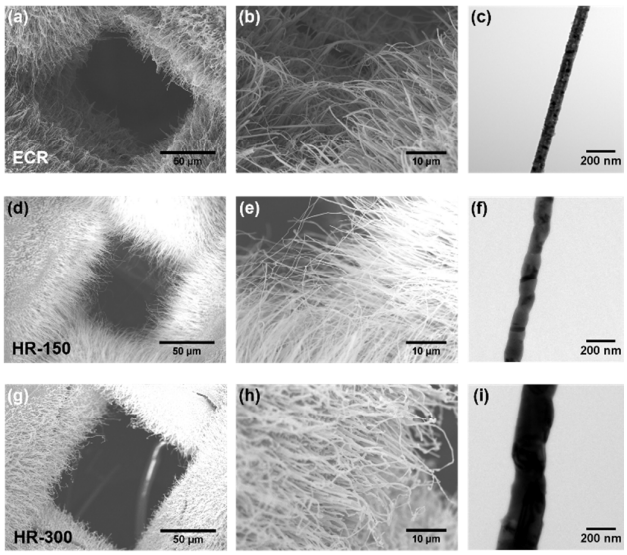

Figure 1. Electron microscopy images of (a-c) ECR, (d-f) HR-150 and (g-i) HR-300 Cu nanowires prepared by reduction of CuO nanowires pre-grown on Cu mesh. The first and second columns are the SEM images, and the right column is TEM images.

Figure 1 presents the electron microscopy images of the three types of Cu nanowires employed in this study, including one prepared by electrochemical reduction (–0.4 V) at room temperature and two prepared by reduction in H_2 at 150 and 300 ^{o}C (denoted as ECR, HR-150 and HR-300, respectively). The ECR nanowires have typical diameters in the range of 50-100 nm and lengths of up to 50 µm (Figure 1 a-c). The HR-150

This journal is © The Royal Society of Chemistry 20xx

Please do not adjust margins

nanowires have similar lengths to the ECR nanowires, but slightly larger diameters of 100-120 nm (Figure 1 d-f). The nanowires prepared at 300 °C have diameters of ≥200 nm and about 20 μm in length (Figure 1 g-i). The larger diameters and shorter lengths of the nanowires prepared at higher temperatures are likely due to thermally driven atomic diffusion and growth of crystalline domains.[32] Corresponding to the nanowire dimensions, the surface roughness factors are estimated to be 356, 145 and 23 (in reference to extended surfaces of polycrystalline Cu electrodes) for the ECR, HR-150 and HR-300 nanowires, respectively, by electrochemical capacitance measurements (see the Experimental methods). It should be pointed out that the smaller roughness factors of the nanowires prepared at higher temperatures may not only be a result of the change in dimensions, but also due to surface smoothing during the thermal reduction treatment.

The electroreduction of CO_2 was studied in a custom-made gas cell containing 0.1 M $KHCO_3$ electrolyte, with the gas- and liquid-phase products analyzed using gas chromatograph-mass spectrometry (GC-MS) and nuclear magnetic resonance (NMR) spectroscopy, respectively. In the high-overpotential region, the total electrode current density per geometric area (J_{tot}, Figure 2a) exhibits a nearly exponential increase as the potential becomes more negative. At -1.0 V, the ECR nanowires reach ~93 mA/cm$^2_{geo}$, compared to ~27 and ~5 mA/cm$^2_{geo}$ for the HR-150 and HR-300 nanowires, respectively. The trend in J_{tot}, ECR > HR-150 > HR-300, is consistent with the trend for surface roughness, suggesting that the different types of Cu nanowires would have rather similar specific activities, namely current density per electrochemically active surface area (ECSA) of Cu (j_{tot}, obtained by dividing J_{tot} with the surface roughness factor). Indeed, the specific activity is determined to be 0.26 and 0.24 mA/cm$^2_{Cu}$ at -1.0 V for the ECR and HR-300 nanowires, respectively, while the HR-150 nanowires have a slightly lower value (0.18 mA/cm$^2_{Cu}$ at -1.0 V) (Figure 2b).

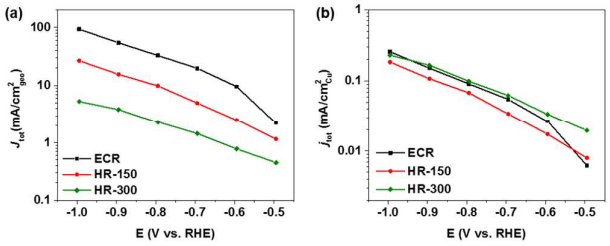

Figure 2. Total current densities generated by the Cu nanowires for CO_2 reduction normalized by (a) the geometric area of the electrode and (b) the ECSA of Cu.

The three types of Cu nanowires exhibit distinct selectivities for CO_2 reduction, with the product distribution dependent on the electrode potential (Figure 3). At -0.5 V, the ECR nanowires have FEs of 53% and 25% toward CO and formate (hydration product of CO), respectively (Figure 3a). CO and formate are also the dominant products from CO_2 reduction on the HR nanowires at this potential, but the FEs of C_1 species (CO + HCOOH) add up to be only 38% and 10% for the HR-150 and HR-300 nanowires, respectively (Figures 3b, c). As the potential becomes more negative, the selectivity increases for multi-carbon products (C_{2+}, including ethylene, ethane, ethanol and 1-propanol), which is associated with the decrease of FEs toward C_1 products, indicating that these (oxygenated) hydrocarbons are formed by further reduction of CO intermediates at elevated overpotentials. The HR-150 nanowires have the highest selectivity toward ethylene (FE_{C2H4}), reaching ~21% at –1.0 V, among the three types of nanowires and throughout the potential region studied here. In addition to these results, it is also noticed that the overall selectivity for CO_2 reduction (FE_{CO2}, counting all the CO_2 reduction products) of the HR-150 nanowires is rather consistent at ~40% throughout the potential region, whereas the ECR and HR-300 nanowires exhibit opposite trends in terms of FE_{CO2} when the potential is scanned from –0.5 to –1.0 V, i.e., decreasing from 82% to 18% for the ECR and increasing from 10% to 38% for the HR-300 nanowires (Figure 3d).

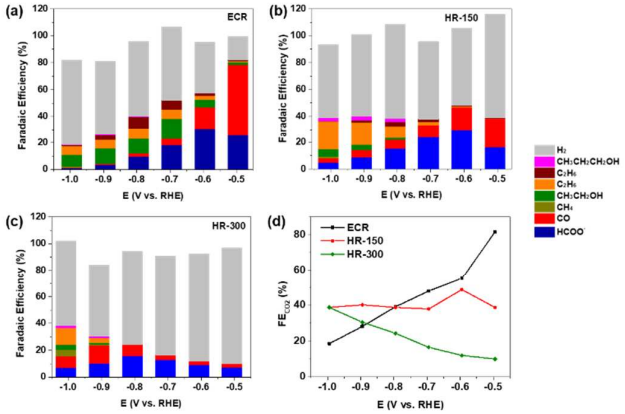

Figure 3. Measured Faradaic efficiencies (FEs) towards the various products for a) ECR, b) HR-150, and c) HR-300 nanowires. (d) Comparison of total FE of CO_2 reduction (FE_{CO2}, counting all the carbon-containing products) for the three types of Cu nanowires.

Our previous work has shown that the nanowires prepared at lower temperatures (e.g., room temperature for the ECR) expose more open facets, such as (100) and (110) (likely also surface defects and stepped sites that are associated with grain boundaries) than those prepared at higher temperatures.[32,33] The energy barriers are known to be lower for CO_2 reduction and C-C bond formation on the open facets (or undercoordinated sites) than on close-packed (111) surfaces.[15–21] The surface-structure sensitivity could thus explain the catalytic performances at relatively low overpotentials where the activity is kinetically limited, such as the trend of ECR > HR-150 > HR-300 for the FE of CO_2 reduction at –0.5 V (Figure 3d). At higher overpotentials where the current density becomes much larger (e.g., J_{tot} > 10 mA/cm$^2_{geo}$ at potentials more negative than –0.6 V for the ECR nanowires, Figure 2a), it is believed that mass transfer effects play a more substantial role in determining the catalytic performance. For example, the lower FEs of CO_2 reduction observed on the ECR nanowires compared to the HR-150 and HR-300 nanowires at –1.0 V can't be explained by the surface

structure effects (Figures 3a-c). Similarly, the decreasing total FE of CO_2 reduction and increasing production of H_2 as the potential becomes more negative observed on the ECR nanowires is hard to be interpreted in terms of kinetic effects, but more likely a result of transport limitations (Figure 3d). The finding that the HR-150 nanowires with an intermediate roughness factor possess the highest selectivity in the high-overpotential region resembles several previous reports on high-surface-area Cu catalysts,[12,31,34] but explicit interpretations of mass transfer effects have not been seen for such nanostructured electrodes.

In the reported study of CO_2 reduction on Cu-poly electrodes, a minimal FE_{H2} (or maximal FE_{CO2}) is observed at ca. −1.1 V.[27] As discussed above, it is likely that the interplay between chemical kinetics on the surface and the transport of CO_2 toward the catalyst has given rise to this volcano-type dependence of FE_{CO2} on the electrode potential: on the right side of the peak, FE_{CO2} increases (or equivalently, FE_{H2} decreases) as the potential becomes more negative owing to the more favorable kinetics of CO_2 reduction than hydrogen evolution (associated with the increase of surface coverage of *CO);[29] on the left side of the peak, FE_{CO2} decreases (or FE_{H2} increases) at more negative potentials, owing to the limited mass transfer of CO_2 toward the catalyst surface at increasing current densities. The peak position is likely at −1.1 V vs. RHE on Cu-poly, but can be dependent on the surface structures, which determines the kinetic competition between CO_2 reduction and hydrogen evolution, and spatial structure of the electrode, including morphology and porosity, as well as the partial pressure of CO_2 and the electrolyte, all of which have an effect on the transport of CO_2 during the reaction. By taking a close look at the electrocatalytic performance of the Cu nanowires (Figures 2a and 3), we further find that the peak position is closely related to the geometric current density of the electrode, which is associated with a current density in the range of 5 – 10 mA/cm^2_{geo} (in the condition of 0.1 M $KHCO_3$, saturated with CO_2 at ~1 atm). This current density range corresponds roughly to the peak position of FE_{CO2} at −0.5 ~ −0.6 V on the ECR nanowires, −0.6 ~ −0.7 V for the HR-150 nanowires, and ~−1.0 V for the HR-300 nanowires. Surprisingly, the current density identified here for the peak FE_{CO2} matches the value observed in the case of Cu-poly, ~8 mA/cm^2_{geo} from the report by Jaramillo *et al.*.[27] This trend is unlikely to be a coincidence, especially considering the different morphologies and surface roughness factors of the two types of electrodes. The relation observed here may still be too preliminary to be claimed universal for CO_2 reduction (even under the given reaction conditions), considering the complexity in comprehensive understanding of the chemical kinetics and mass transfer on the nanostructured electrodes, but we believe it is an important feature of the CO_2 reduction on high-surface-area, nanostructured electrocatalysts and certainly deserves more detailed studies in the future.

To develop a more comprehensive understanding of the mass transfer effects in CO_2 reduction electrocatalysis, we have plotted the overall current densities of CO_2 reduction (excluding the partial currents toward hydrogen evolution) against the electrode potentials for the three types of Cu nanowires, both per geometric area of the electrode (J_{CO2}, Figure 4a) and per ECSA of Cu (j_{CO2}, Figure 4b). It can be seen that J_{CO2} exhibits a monotonous increase as the potential becomes more negative for all the three types of nanowires, following the order ECR > HR-150 > HR-300 throughout the potential region, which is consistent with the trend for roughness factors (Figure 4a). However, different situations are observed for the current densities per ECSA, where the ECR nanowires have the highest j_{CO2} at potentials more positive than -0.8 V but the HR-150 nanowires outperform at more negative potentials (Figure 4b). The lower j_{CO2} of the ECR nanowires at -0.9 and -1.0 V is clear indication of CO_2 diffusion limitation, which is well correlated to the lower FEs of this type of nanowires than the other two types for the reaction in this potential region (Figure 3).

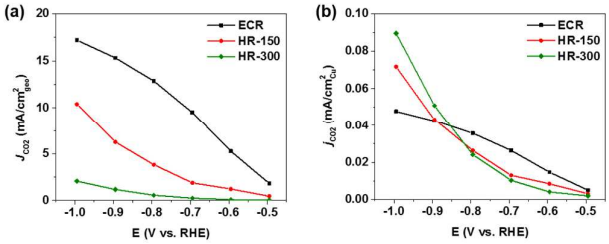

Figure 4. Comparison of CO_2 reduction current densities (a) per geometric area and (b) per ECSA of Cu at different electrode potentials for the three types of Cu nanowires.

We have recently developed a transport model for the CO_2 reduction reaction on Cu nanowire electrocatalysts.[30] Compared to the previously reported simulations for planar electrodes,[22] our model has taken into account the spatial distribution of reactions (including CO_2 reduction toward various products and hydrogen evolution) along the nanowires, by assuming a first-order dependence of the CO_2 reduction reaction activity on the local concentration of CO_2 and a linear increase of the hydrogen evolution reaction activity with the depth into the nanowires. This has allowed us to simulate the surface concentrations of chemical species and local pH along the nanowires at each potential (see the Supporting Information, section 3). Figure 5a summarizes the obtained CO_2 concentration ($[CO_2]_{surface}$) on the electrode surface (base of the nanowires) at various potentials, taking into account the nanowire lengths. It can be seen that, for the three types of Cu nanowires, $[CO_2]_{surface}$ decreases as the potential becomes more negative, with the magnitude of the drop below the bulk value following the trend ECR > HR-150 > HR-300. In particular, it approaches zero at -0.9 V on the ECR nanowires. The complete depletion of CO_2 on the electrode surface at the high-overpotential limit, or more relevantly, the large current density (ca. >15 mA/cm^2_{geo}, Figure 4a), is indicative of the diffusion limitation, as confirmed by the observation of a plateau in the CO_2 conversion rate, calculated from the experimental data, in this potential region (Figure 5b, see more details of the calculation in the Supporting Information, section 4). The observation that the FEs of CO_2 reduction drop as the potential becomes more negative for the

This journal is © The Royal Society of Chemistry 20xx

Please do not adjust margins

ECR nanowires (Figure 3a) can thus be attributed to the evolution of more hydrogen as the reaction approaches or goes beyond the diffusion limitation of CO_2. In contrast, the surface concentration of CO_2 on the HR-300 nanowires is nearly the same as in the bulk electrolyte, indicating that the reaction is not limited by CO_2 diffusion and the conversion for CO_2 flux is low in this case. The HR-150 nanowires display more CO_2 depletion than the HR-300, but does not reach complete depletion of CO_2 even at -1.0 V. These results explain the observed trends for FE_{CO2} in Figure 3d, namely the rather consistent total selectivity for CO_2 reduction throughout the potential region for the HR-150 nanowires, whereas the ECR and HR-300 nanowires exhibit opposite trends. It is noticed that the trapping of gaseous species (e.g., CO) inside porous electrocatalysts has been reported to be beneficial for enhancing the selectivity toward C_2 products, due to the increased residence time of reaction intermediates.[12,35] If the Cu nanowires also possess such a trapping effect (which remains unclear), the HR-150 nanowires with an intermediate roughness could have also reached a balance between the supply of CO_2 and the retention of intermediates for the reaction, giving rise to the highest selectivity toward ethylene at the high-overpotential (or, large-current density) conditions.

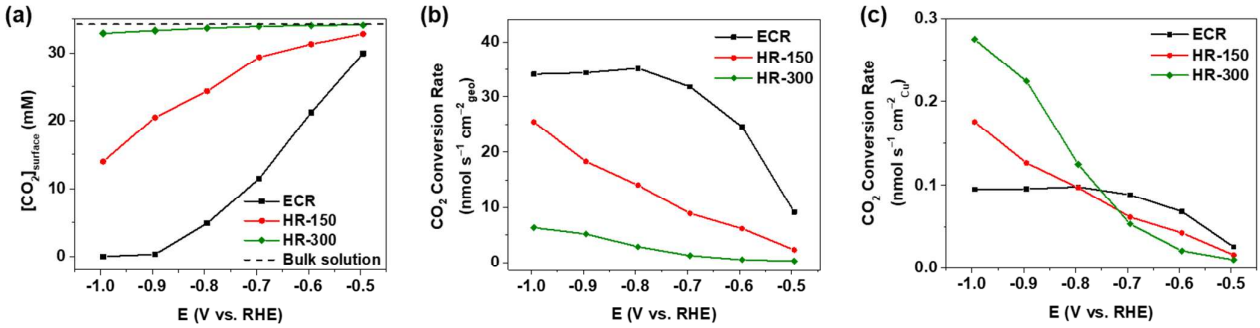

Figure 5. (a) Simulated surface concentration of CO_2 (at the base of the Cu nanowires) in dependence of the electrode potential. (b, c) CO_2 conversion rates per geometric area of the electrode (b) and per ECSA of Cu (c) calculated based on the experimentally measured current densities and FEs (as shown in Figures 2 and 3).

From the above discussion, we can see that the mass transfer effects place a physical limitation on the rate of CO_2 conversion on the nanowire electrocatalysts. This value is determined to be ~35 nmol s^{-1} cm^{-2}_{geo} and ~0.10 nmol s^{-1} cm^{-2}_{Cu} from the calculated CO_2 conversion rates (Figures 5b and c). It should be pointed out that the theoretical diffusion limit is estimated to be ca. 113 nmol s^{-2} cm^{-2} according to the Fick's law, as determined by the concentration and diffusivity of CO_2 in the electrolyte (see section 3 in the Supporting Information). This theoretical limit corresponds to ~0.32 nmol s^{-1} cm^{-2}_{Cu} considering the roughness factor (356) of the ECR nanowires. The smaller values of maximal CO_2 conversion rates seen from the electrocatalytic studies suggest that the diffusion of CO_2 through the Cu nanowires may also be subjected to other restrictions, such as the higher local pH in the space among the nanowires that has reduced the concentration of dissolved CO_2. Similar arguments could also be made for the complete depletion of CO_2 at the base of the ECR nanowires at high overpotentials (as mentioned above), namely the attainability of CO_2 on the electrode surface may not only be limited by the reaction and consumption of CO_2 along the nanowires, but also by the rise of local pH that has further attenuated the supply of $_{CO2.}$[30] Compared to the ECR nanowires, the HR-150 nanowires have a lower CO_2 conversion rate of ~25 nmol s^{-1} cm^{-2}_{geo} at -1.0 V (Figure 5b). This indicates that an even higher J_{CO2} could be reached by the HR-150 nanowires if the potential is more negative than -1.0 V. The HR-300 nanowires have the highest CO_2 conversion rate per ECSA, reaching 0.28 nmol s^{-1} cm^{-2}_{Cu} at -1.0 V (Figure 5c). Considering that the HR-300 nanowires have the lowest roughness factor in the series, their higher specific activity (j_{CO2}, Figure 4b) at this potential is simply a result of being less limited by CO_2 diffusion, instead of indicating the presence of more active sites or higher turnover rates.

Conclusions

In summary, we have studied the electroreduction of CO_2 on high-surface-area Cu electrocatalysts. At the relatively high overpotentials (from -0.5 to -1.0 V), mass transfer is found to play an important role in determining the electrocatalytic performance owing to the large current densities (ca. -1 – -100 mA/cm^2_{geo}). The limited supply of CO_2 places an upper limit on the CO_2 conversion rate and causes a drop in Faradaic efficiency for CO_2 reduction at large current densities. As a result, the Cu nanowires with intermediate surface roughness (HR-150) has the best performance among the three types of high-surface-area electrocatalysts investigated here. Our work highlights the importance of taking transport into account in the design of high-performance electrodes for CO_2 reduction.

Conflicts of interest

There are no conflicts to declare.

Acknowledgements

This work was supported by the National Science Foundation (CHE-1437396) and the Discovery Award of Johns Hopkins University. This study made use of the Johns Hopkins University Department of Chemistry Core Facilities and the authors would like to acknowledge the NMR manager Dr. Joel A. Tang for his assistance.

Notes and references

1 G. A. Olah, G. K. S. Prakash and A. Goeppert, *J. Am. Chem. Soc.*, 2011, **133**, 12881–12898.
2 D. T. Whipple and P. J. A. Kenis, *J. Phys. Chem. Lett.*, 2010, **1**, 3451–3458.
3 M. R. Singh, E. L. Clark and A. T. Bell, *Proc. Natl. Acad. Sci.*, 2015, **112**, E6111–E6118.
4 Y. Hori, K. Kikuchi and S. Suzuki, *Chem. Lett.*, 1985, **14**, 1695–1698.
5 Y. Hori, A. Murata and R. Takahashi, *J. Chem. Soc.-Faraday Trans. I*, 1989, **85**, 2309–2326.
6 Y. Hori, *Mod. Asp. Electrochem. No 42*, 2008, 89–189.
7 M. Gattrell, N. Gupta and A. Co, *J. Electroanal. Chem.*, 2006, **594**, 1–19.
8 C. W. Li and M. W. Kanan, *J. Am. Chem. Soc.*, 2012, **134**, 7231–7234.
9 R. Reske, H. Mistry, F. Behafarid, B. Roldan Cuenya and P. Strasser, *J. Am. Chem. Soc.*, 2014, **136**, 6978–6986.
10 D. Raciti, K. J. Livi and C. Wang, *Nano Lett.*, 2015, **15**, 6829–6835.
11 A. S. Hall, Y. Yoon, A. Wuttig and Y. Surendranath, *J. Am. Chem. Soc.*, 2015, **137**, 14834–14837.
12 A. Dutta, M. Rahaman, N. C. Luedi, M. Mohos and P. Broekmann, *ACS Catal.*, 2016, **6**, 3804–3814.
13 D. Kim, J. Resasco, Y. Yu, A. M. Asiri and P. Yang, *Nat. Commun.*, 2014, **5**, 4948.
14 J. P. Grote, A. R. Zeradjanin, S. Cherevko, A. Savan, B. Breitbach, A. Ludwig and K. J. J. Mayrhofer, *J. Catal.*, 2016, **343**, 248–256.
15 Y. Hori, H. Wakebe, T. Tsukamoto and O. Koga, *Surf. Sci.*, 1995, **335**, 258–263.
16 K. J. P. Schouten, Z. Qin, E. P. Gallent and M. T. M. Koper, *J. Am. Chem. Soc.*, 2012, **134**, 9864–9867.
17 F. Calle-Vallejo and M. T. M. Koper, *Angew. Chem. Int. Ed.*, 2013, **52**, 7282–7285.
18 J. H. Montoya, C. Shi, K. Chan and J. K. Nørskov, *J. Phys. Chem. Lett.*, 2015, **6**, 2032–2037.
19 Y. Hori, I. Takahashi, O. Koga and N. Hoshi, *J. Phys. Chem. B*, 2002, **106**, 15–17.
20 I. Takahashi, O. Koga, N. Hoshi and Y. Hori, *J. Electroanal. Chem.*, 2002, **533**, 135–143.
21 W. J. Durand, A. A. Peterson, F. Studt, F. Abild-Pedersen and J. K. Nørskov, *Surf. Sci.*, 2011, **605**, 1354–1359.
22 N. Gupta, M. Gattrell and B. MacDougall, *J. Appl. Electrochem.*, 2006, **36**, 161–172.
23 R. Kas, R. Kortlever, H. Yılmaz, M. T. M. Koper and G. Mul, *ChemElectroChem*, 2015, **2**, 354–358.
24 M. R. Singh, E. L. Clark and A. T. Bell, *Phys. Chem. Chem. Phys.*, 2015, **17**, 18924–18936.
25 A. S. Varela, M. Kroschel, T. Reier and P. Strasser, *Catal. Today*, 2016, **260**, 8–13.
26 M. R. Singh, Y. Kwon, Y. Lum, J. W. Ager and A. T. Bell, *J. Am. Chem. Soc.*, 2016, **138**, 13006–13012.
27 K. P. Kuhl, E. R. Cave, D. N. Abram and T. F. Jaramillo, *Energy Environ. Sci.*, 2012, **5**, 7050–7059.
28 Y.-J. Zhang, V. Sethuraman, R. Michalsky and A. A. Peterson, *ACS Catal.*, 2014, **4**, 3742–3748.
29 H. Ooka, M. C. Figueiredo and M. T. M. Koper, *Langmuir*, 2017, **33**, 9307–9313.
30 D. Raciti, M. Mao and C. Wang, *Nanotechnology*, 2018, **29**, 044001.
31 H. Mistry, A. S. Varela, C. S. Bonifacio, I. Zegkinoglou, I. Sinev, Y.-W. Choi, K. Kisslinger, E. A. Stach, J. C. Yang, P. Strasser and B. R. Cuenya, *Nat. Commun.*, 2016, **7**, 12123.
32 L. Cao, D. Raciti, C. Li, K. J. T. Livi, P. F. Rottmann, K. J. Hemker, T. Mueller and C. Wang, *ACS Catal.*, 2017, **7**, 8578–8587.
33 D. Raciti, L. Cao, K. J. T. Livi, P. F. Rottmann, X. Tang, C. Li, Z. Hicks, K. H. Bowen, K. J. Hemker, T. Mueller and C. Wang, *ACS Catal.*, 2017, **7**, 4467–4472.
34 M. Ma, K. Djanashvili and W. A. Smith, *Angew. Chem. Int. Ed.*, 2016, **55**, 6680–6684.
35 A. Dutta, M. Rahaman, M. Mohos, A. Zanetti and P. Broekmann, *ACS Catal.*, 2017, **7**, 5431–5437.

This journal is © The Royal Society of Chemistry 20xx

Catalysis Science & Technology

ARTICLE

Mass Transfer Effects in CO_2 Reduction on Cu Nanowire Electrocatalysts

Table of Content

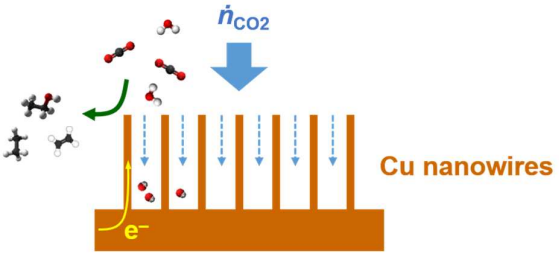

Mass transfer effects play an important role in CO_2 electroreduction, giving diffusion-limited activity and selectivity on Cu nanowire electrocatalysts.

[a] *Department of Chemical and Biomolecular Engineering, Johns Hopkins University, Baltimore, Maryland 21218*
* Email: chaowang@jhu.edu
Electronic Supplementary Information (ESI) available: [details of any supplementary information available should be included here]. See DOI: 10.1039/x0xx00000x

This journal is © The Royal Society of Chemistry 20xx